

Design and Control of a Novel High Payload Light Arm for Heavy Aerial Manipulation Tasks

Michele Marolla, Jonathan Cacace^a and Vincenzo Lippiello^b

CREATE Consortium and PRISMA Lab, Department of Engineering and Information Technology,
University of Naples Federico II, via Claudio 21, Naples, Italy

Keywords: Aerial Manipulation, Robotic Arm, Inspection and Maintenance.

Abstract: Aerial manipulation is a rapidly emerging research field that explores the use of Unmanned Aerial Vehicles as mobile manipulators. To enable aerial manipulation, UAVs must be equipped with lightweight robotic arms capable of interacting with the environment. However, due to battery life constraints and payload limitations, these arms must be designed to be as light as possible, which restricts their ability to transport and manipulate heavy objects. In this work, we introduce a novel aerial manipulator prototype designed specifically for high payload manipulation. The arm is designed to have its center of mass as close as possible to its base, which is attached to the aerial frame. The arm incorporates a system of belts to facilitate the movement of its various joints. This paper presents the arm's design, along with a control approach to compensate for the elasticity introduced by the belts. To showcase the system's capabilities, we conduct two sets of experiments. Firstly, the arm is tested within a controlled laboratory environment. Secondly, we deploy an aerial robot equipped with the proposed prototype in a powerline maintenance task.


1 INTRODUCTION


Over the past decade, the utilization of Unmanned Aerial Vehicles (UAVs) has seen remarkable success across various industries and applications. UAVs have been effectively employed in diverse fields including search and rescue operations (Cacace et al., 2016) (Sibanyoni et al., 2019) (Mishra et al., 2020), industrial building inspection (Cacace et al., 2013), inspection and maintenance tasks (Uzakov et al., 2020) (Tosato et al., 2019), surveillance, remote sensing, and more. Notably, there has been a recent advancement in aerial systems that enables them to undertake operations involving direct interaction with the environment, such as grasping and piercing (Ruggiero et al., 2018). This development has proven invaluable in handling industrial and service applications that are either deemed hazardous or too intricate for human operators. The evolution of aerial manipulation capabilities has led to the introduction of a wide array of platforms (Ollero et al., 2022), ranging from fixed propeller configurations (Cano et al., 2014) (Tognon et al., 2019) to tilting (Tognon et al., 2019) or tilted multi-copters (Franchi, 2019). Re-



Figure 1: Proposed manipulator mounted under an Unmanned Aerial Vehicle during an electrical power line maintenance task.

gardless of the actuation type, the aerial manipulators share a critical component: their robotic arm. A fundamental concern in aerial manipulation is striking a balance between the arm's functionality and the constraints imposed by the UAV's battery life and pay-

^a  <https://orcid.org/0000-0002-1639-5655>

^b  <https://orcid.org/0000-0002-6089-2333>

load limitations. Achieving optimal performance requires designing lightweight robotic arms that retain adequate strength and dexterity. This delicate trade-off between weight and capability presents a substantial challenge, as lighter arms may encounter difficulties in efficiently transporting and manipulating heavier objects. Overcoming this limitation is essential for broadening the scope of tasks that aerial manipulators can effectively accomplish. Recent advancements in Aerial Manipulation Robots have showcased their capability to perform diverse operations, such as object grasping (Suarez et al., 2018), sensor installation and retrieval (Suarez et al., 2020), contact-based inspection (Trujillo et al., 2019), and execution of various tasks using grippers and other tools (Shimahara et al., 2016). The integration of these manipulators in multi-rotors has led to the development of numerous prototypes, including multijoint arms (Bellicoso et al., 2015), dual-arm systems (Suarez et al., 2018), linear actuators (Hamaza et al., 2019), delta manipulators (Chermprayong et al., 2019), compliant joint arms (Suarez et al., 2020), long-reach aerial manipulators (Miyazaki et al., 2020), and even three-arm manipulators that serve both as object grippers and reconfigurable landing gear (Paul et al., 2019). For an aerial manipulation robot to efficiently interact with the environment, it must possess two crucial characteristics: a lightweight structure and a high payload lifting capacity. For this reason, we propose the development and experimental validation of a new morphology of an aerial manipulation robot arm consisting of extremely light structure, capable of lifting and manipulating a heavy weight (See Figure 1). The actuation mechanism is based on a group of belts for the first joints and a group of servo motors for the arm wrist. The belt system has been chosen to allow the placement of the main motor group close to the base of the arm. However, the presence of the belts induces elasticity in the arm motion, particularly when it is stretched. For this reason, a control technique exploiting a couple of inertial sensors placed on the arm structure is used to compensate such elasticity, improving the precision of the end effector during the operations.

The prototype's effectiveness has been demonstrated through two comprehensive tests. The initial test focused on assessing the elasticity compensation controller in a controlled laboratory setting. By comparing the arm's motion with and without the compensation, the objective was to evaluate its performance. The second test took place in a test bed facility, where the arm was integrated into an aerial system. During this test, a maintenance task involving an electrical power line was successfully executed,

showcasing the arm's practical functionality under real-world conditions.

To summarize, this work presents significant contributions, including (i) The development of an innovative lightweight manipulator designed specifically for aerial manipulation tasks, featuring remarkable payload lifting capabilities. This design ensures optimal performance while adhering to the weight constraints imposed by aerial systems. (ii) The introduction of a control approach aimed at effectively compensating for elasticity in the proposed arm during motion tasks. This compensatory mechanism enhances the precision and stability of the arm's movements, thereby improving its overall performance.

The rest of the paper is organized as follows. In Section 2 the motivational use case in which the proposed solution has been used is described. In Section 3 the mechanical and electrical specifications of the arm are discussed and in Section 4 the arm elasticity compensation is introduced. The software architecture to control the proposed arm is presented in Section 5. Finally, the system at work is shown in Section 6. Finally, we include an appendix section to report the hardware adopted in the design of the arm.

2 MOTIVATION

This work is primarily motivated by the need for high payload manipulation in various tasks prevalent today. Particularly, it draws inspiration from the experimental use case proposed by the Aerial-Core (AERIAL COgnitive integrated multi-task Robotic system with Extended operation range and safety) H2020 project (Cacace and et al., 2021). The project aims to leverage the flying capabilities of UAVs for inspecting and maintaining power grids, involving activities such as landing and perching on energy lines, as depicted in Figure 1. The tasks entail installing and removing various devices from the power lines (IEEE, 2009), including bird diverters (helical and clip diverters) used to prevent bird collisions, which pose a threat to both avian life and the power infrastructure or electrical cable spacers. Additionally, the power lines are exploited to improve the efficiency of the aerial system. In particular, a recharging stations may need to be installed to extend the UAVs' battery life. These tasks often require specialized end-effectors and introduce additional payload to the robotic arm. For instance, a tool to carry out helical bird diverter manipulation is presented in (Cacace et al., 2023). In particular, in the latter work, a unique tool specifically designed to remove helical bird diverters from power lines.

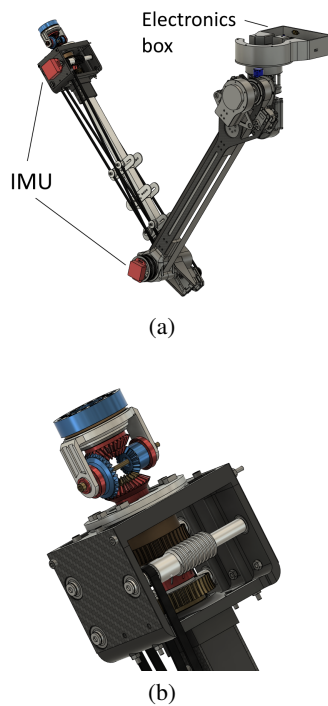


Figure 2: Overview of the proposed arm with (a) the IMU sensors and (b) detail of the spherical wrist.

Another approach to addressing general power lines maintenance is discussed in the work by (Suarez et al., 2023). They propose a lightweight dual arm system that can be transported along the power line to perform maintenance operations. However, it is important to note that the payload capacity and force exerted by their device are relatively low compared to the solution proposed in this work.

3 MANIPULATOR DESIGN

The main objective of this paper is to showcase the development of an articulated robotic arm capable of executing various demanding tasks in multiple aerial manipulation scenarios. These tasks encompass object grasping, device installation and retrieval, contact-based inspection, and more.

The manipulator proposed in this work is an anthropomorphic arm featuring six Degrees of Freedom (DoFs), accompanied by a gear-based spherical wrist that serves as the end effector. This configuration is essential to achieve a superior level of dexterity, enabling the arm to successfully accomplish all the designated tasks. The last joint of the arm has been thoughtfully designed with a versatile flange, allowing for easy attachment of different end-effectors specifically tailored to carry out specific tasks.

The proposed robotic arm has been designed to weigh 3 kg, making it lightweight and agile. Despite its compact size, it boasts an impressive payload capacity of 5 kg when fully extended. This remarkable payload/weight ratio of $1.67 > 1$ sets it apart from other similar solutions proposed in the literature.

The ability to achieve such a high payload/weight ratio is a crucial and distinguishing feature of this robotic arm. It enables the arm to be effectively deployed on aerial systems, where tasks often require either substantial interaction forces or the handling of heavy payloads. By surpassing the payload/weight ratios of alternative solutions found in the literature, this arm proves to be an exceptional choice for aerial manipulation scenarios that demand both robust force application and efficient payload transport.

However, due to the high payload/weight ratio, the resultant arm motion is quite limited. Specifically, the maximum velocity achievable by the end-effector is within the range of 5 to 20 cm/s, depending on the specific configuration of the arm. While this may impose some constraints, it is important to note that the primary application scenario where the proposed solution excels is when the aerial system is perched on a surface before initiating the manipulation task. The design of the arm takes inspiration from the Haddington Dynamics Dexter HDI ¹, with notable modifications tailored to enhance its performance. One significant alteration involves the placement of one of the motors responsible for controlling the wrists. This motor has been strategically positioned in line with the connection between the first and second link, as illustrated in Figure 3b. This design serves multiple purposes. Firstly, it enables a more balanced and even distribution of the arm's weight, ensuring optimal stability during operation. Secondly, by eliminating the need for additional components such as belts, pulleys, and bearings, the overall weight of the arm is significantly reduced. This reconfiguration of the wrist motor placement not only improves weight distribution, but also contributes to a more efficient and streamlined design. The reduction in the number of components leads to enhanced reliability and ease of maintenance. Additionally, it allows for a more compact and lightweight robotic arm without compromising on its strength and functionality.

There are other systems available in the market that share similarities with the one proposed in this work. One notable example is the Dexter HDI, introduced earlier, and another comparable system is the UR3 from Universal Robots ². In order to pro-

¹<https://www.hdrobotic.com/>

²<https://www.universal-robots.com/products/ur3-robot/>

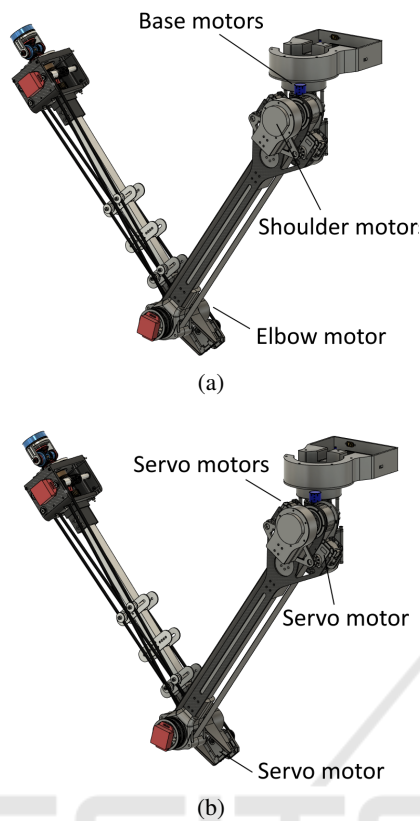


Figure 3: Motor disposition along the arm. (a) Brushless motors for the arm, (b) servo motors for the wrist.

vide a comprehensive analysis, Table 1 compares the proposed arm with these commercial robotic arms. It is important to note that while the proposed arm may have certain disadvantages in specific application areas, it remains competitive, particularly in terms of payload capacity. It is worth acknowledging that the proposed solution competes favorably in the market, despite being potentially disadvantaged in certain comparison aspects due to the nature of its particular application area. The focus on payload capacity is a strength of the proposed arm, enabling it to excel in tasks requiring substantial payload handling. In addition, the proposed solution is lighter (to be transported from an aerial system) and the power requirement is lower.

3.1 Mechanical Description

The arm has been designed considering two kinds of motors, depending on the type of joint to control and the demanded torque. In particular, the first three motors are brushless motors, while the spherical wrist is composed of three servo motors (see Fig. 3). Also, the actuation type depends on the positioning of the motor along the arm structure and, in particular, the

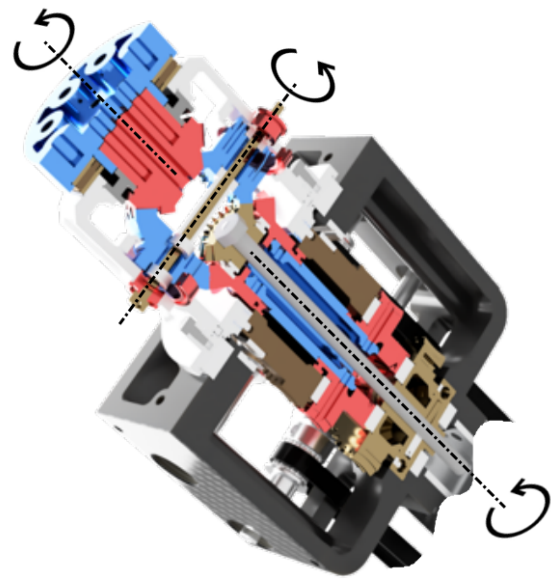


Figure 4: Cad section of the spherical wrist design.

first joint is actuated directly by the motor, and the link is attached to the motor's output flange. The second joint is actuated by the motor coupled with a harmonic drive transmission to guarantee a reduction ratio of 1:100. Finally, the third joint is actuated by the motor coupled with a harmonic drive transmission to guarantee a reduction ratio of 1:80, while it uses a belt-pulley mechanism to actuate the forearm. During the design process, the FEA (Finite Element Analysis) has been conducted. Each part of the arm has been designed with the same approach, using a first layer forming the structure of the overall dimensions, and a second layer made by a thin element realized in strong material (carbon fiber or aluminum). This provides structural resistance to the robot, while guaranteeing at the same time the required lightness. The analysis demonstrated that carbon fiber layers work properly, absorbing a great part of the stress. As for the spherical wrist, it has been designed in steel and a section is shown in Figure 4. The three wrist joints are actuated using servomotors and belts.

3.2 Electrical Description

The power unit of the robotic arm is thoughtfully integrated within the manipulator base, contributing to a neat and self-contained system. To activate the arm, a 24 V power supply unit is required, providing the necessary electrical energy. In terms of communication, the arm establishes an Ethernet connection with an external controller, typically a standard laptop. This communication link allows for seamless interaction and control of the arm's operations. Further informa-

Table 1: Comparison between commercial robot arms and the proposed solution.

	Dexter HDI		UR3e		Proposed arm	
Robot weight [kg]	6		11.2		3	
Reach [mm]	700		500		700	
Payload [kg]	3		3		5	
Power requirements [W]	40 - 100		100 - 300		50	
Joint ranges [deg]	Base	360	Base	360	Base	360
	Pivot	270	Shoulder	360	Shoulder	180
	Shoulder	270	Wrist1	360	Elbow	270
	Differential	180	Wrist2	360	Wrist1	360
	Differential	360	Wrist3	360	Wrist2	360
	Gripper	300			Wrist3	360
End effector included	Yes		No		No	

tion regarding the system architecture can be found in Section 5.

The firmware implementation, responsible for directly controlling the hardware, is executed on an on-board microcontroller. This microcontroller efficiently handles communication with the motors and sensors, ensuring accurate and real-time control of the arm's movements. To consolidate the electronic components and optimize space utilization, a compact custom-made Printed Circuit Board (PCB) is employed, providing a centralized platform for the necessary electronics. Additionally, a fuse is incorporated into the system design to protect against short-circuits, promptly interrupting the power supply in such instances and safeguarding the overall system.

As previously mentioned, the arm has been designed with versatility in mind, enabling it to work with various tools and end-effectors. To facilitate effortless integration of these tools, their servomotors can be easily connected in a daisy-chain configuration to the wrist control motors. The microcontroller intelligently detects and manages these connected tools, allowing for seamless switching between different tools during operation. This flexibility and modularity enhance the arm's adaptability to diverse task requirements.

Furthermore, the arm incorporates two Inertial Measurement Units (IMUs), strategically placed on the wrist and elbow. These IMUs provide valuable data to the microcontroller, which utilizes it to compensate for elasticity caused by the belts and the high payload of the arm. By actively compensating for elasticity, the arm achieves more precise and accurate movements, ensuring optimal performance. For a more comprehensive understanding of the elasticity compensation method employed, refer to Section 4 for detailed information.

4 ELASTICITY COMPENSATION

As already stated, the utilization of belt transmissions in the arm introduces inherent challenges related to elasticity. While transient behavior can be tolerated due to the arm's limited velocity, steady-state errors may still occur. These errors become more pronounced as the payload weight increases and the arm extends further. Given that the proposed arm is specifically designed for heavy tasks, such as manipulating objects weighing up to 5 kg, it is imperative to address this issue. Failure to do so can result in significant displacement of the end effector caused by elasticity, rendering it incapable of autonomously executing assigned motion tasks.

To tackle this problem, our solution incorporates two IMUs strategically positioned on the wrist and elbow of the arm. These IMUs are installed at the end of the second and third links of the arm, as depicted in Figure 2 (a). By leveraging the data provided by these IMUs, it becomes possible to accurately calculate the real orientation of the arm's links and the precise position of the end effector. This information enables the implementation of corrective measures, allowing the arm to successfully execute tasks even in the presence of elasticity.

Given that the arm motors are controlled in velocity, the computation of the commanded velocity for the i -th motor is based on the desired position $q_{d,i}$ of the i -th link and the current position q_i^m measured by the motor's encoder.

$$v_{d,i} = G_{r,i} * K_{p,i} * \tilde{q}_i \quad (1)$$

where $G_{r,i}$ is the gear ratio of the transmission linked to the motor i , $K_{p,i}$ is a proportional gain conveniently tuned, and $\tilde{q}_i = q_{d,i} - q_i^m$ is the error between the desired link orientation and the orientation given by the

motor encoder also considering the mechanical transmission.

Due to the elasticity, the real orientation q_i of the i -th link is different from the q_i^m read by the motor's encoder. For this reason, there will be an error at steady-state that the system is not aware of. Consider now the value q_i^i read by the IMU: this represents the real orientation of the i -th link.

The equation of the commanded velocity becomes:

$$v_{d,i} = G_{r,i} * K_{p,i} * \tilde{q}_i \quad (2)$$

where $\tilde{q}_i = q_{d,i} - q_i^i$ is the error between the desired orientation and the one read by the IMU. The implementation of elasticity compensation, as previously described, is executed on the on-board microcontroller and can be activated or deactivated through commands sent by the main companion computer. By adopting this approach, the correction algorithm remains transparent to the high-level controller and trajectory planner, allowing for seamless integration into the overall system. The microcontroller takes charge of establishing communication with the IMUs and applies a low-pass filter to the measurements obtained from them. This filtering process helps to refine the accuracy of the data used for elasticity compensation. Additionally, a security layer is incorporated to handle potential issues such as missing or noisy measurements from the IMUs. If such situations occur, the security layer activates, halting the correction algorithm and reverting back to the standard controller. This implementation of elasticity compensation has proven to be highly effective in mitigating the effects of elasticity caused by high payloads. It ensures the arm is capable of successfully accomplishing the required tasks, as discussed in Section 6. By enabling precise and reliable compensation, the arm can maintain the desired trajectory and achieve the desired level of performance.

5 SYSTEM ARCHITECTURE

This section provides an overview of the system architecture implemented to successfully control the arm. The architecture comprises two main layers, each serving a specific purpose, and is outlined in Figure 5.

The first layer consists of the Controllers, which are implemented on an external companion computer running a standard GNU/Linux operating system. This layer leverages the Robot Operating System (ROS) (Joseph and Cacace, 2018) as the robotic middleware. Within this layer, two distinct types of controllers have been developed. The first controller enables motion control in the arm's joint space,

known as Direct Joint Control. It allows precise control over individual joints, facilitating intricate movements. The second controller enables control of the arm in the operational space, known as Inverse Kinetic Control. This controller utilizes the Kinematics and Dynamics Library (KDL), enabling precise control of the arm's position and orientation in the operational space.

At a lower level, the system hardware is controlled by a custom firmware installed on a microcontroller. This firmware is responsible for implementing the communication protocol with the brushless and servo motors used in the arm. Through this communication protocol, the firmware allows commanding the position and velocity of the motors, while retrieving their current state as output. In addition to motor control, this layer incorporates essential safety checks to ensure compliance with joint and velocity limits, preventing any potential violations. Furthermore, this layer includes a configuration storage system, which stores a set of pre-planned configurations. These configurations are utilized to set up the arm for different operations, such as an initial manipulation configuration or a closing transporting configuration. In addition, in this layer are implemented all the needed value transformation to translate joint commands into motor commands, taking into account gear ratios and motor coupling.

To establish communication between the companion computer and the microcontroller, a custom network interface is employed. This network interface utilizes an Ethernet connection, facilitating reliable and efficient data transmission between the two components of the system.

The hardware chosen for the development of the mechatronic system is listed in the following.

- Three T-Motor motors Ak60 have been selected for the first three elements of the arm. The communication protocol has been implemented using the CAN standard
- The spherical wrist is composed of Dynamixel MX28-AT 2.0 servomotors, communicating with the RS485 protocol
- The WitMotion WT61C inertial sensors have been used for the elasticity compensation, with the TTL communication protocol.
- The microcontroller connecting the compound computer and the system hardware is based on the ST STM32F767ZI microcontroller

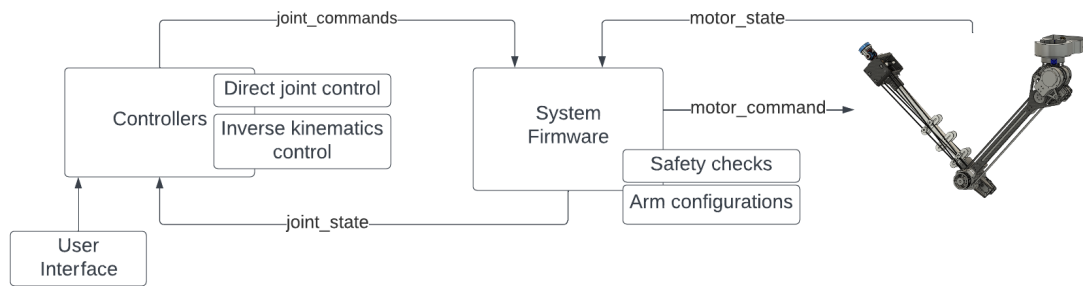


Figure 5: System architecture.

6 EXPERIMENTS

The system under examination has been tested in two different operational scenarios, each providing different insights into its performance and capabilities.

In the first case, the arm was subjected to testing within a controlled indoor facility. This facility was equipped with an OptiTrack³ motion capture system, used to accurately track the arm's movements. By employing this motion capture system, the position of the manipulator's end-effector relative to its base throughout various motions has been tracked. As for the second test case, the arm has been tested in a real-world experiment. In this scenario, the arm was positioned downward in an aerial system that was perched over a power line cable. This setup aimed to simulate a practical application where the arm needed to be deployed in an elevated and potentially hazardous environment.

A video showing the execution of those experiments can be found at: <http://y2u.be/vDPNLvIjPpo>.

6.1 Case Study 1

In this particular test case, the robotic arm was firmly secured to a stable ground structure to eliminate any external factors that could affect its motion. To simulate a practical scenario, a device weighing 2 kg was

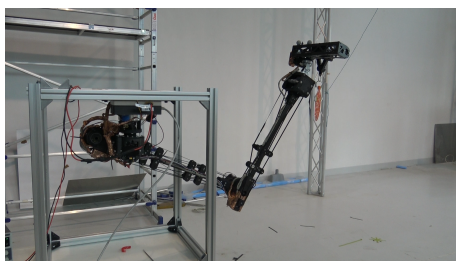


Figure 6: Laboratory site to test the proposed manipulator in the elasticity compensation task.

³<https://optitrack.com/>

attached to the end effector of the arm. This additional payload introduces challenges related to elasticity and requires effective compensation strategies to maintain precise control.

To assess the performance of the control approach, an operational space trajectory consisting of four waypoints was planned. To ensure smooth and continuous motion, a fifth-order spline was used to interpolate between the waypoints. The trajectory was executed twice: once with the elasticity compensation enabled and once without it. This comparative analysis enables a direct evaluation of the impact of the compensation technique on the arm's ability to accurately follow the desired trajectory.

During the motion task, the OptiTrack motion capture system was employed to track the position of the end effector relative to the base frame of the arm. This high-precision tracking system provides accurate and reliable measurements of the arm's actual motion.

The results of the motion capture system were analyzed and compared between the two modalities, with and without elasticity compensation. Figure 7 illustrates the recorded motion displacement, clearly highlighting the differences between the compensated and uncompensated motions. Notably, the z-axis,

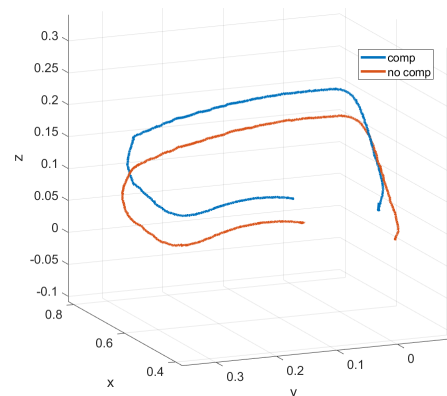


Figure 7: Laboratory test using a motion capture system to estimate the effect of the elasticity compensation during the operations.

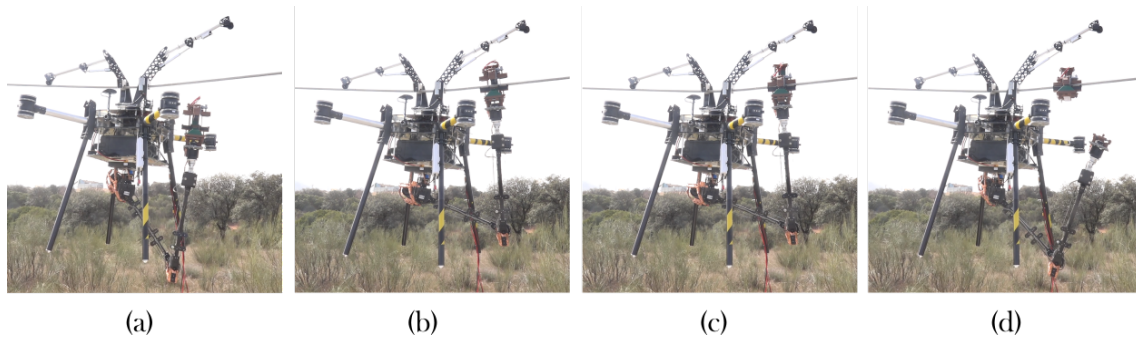


Figure 8: Real world experiment tests case: installation of a particular tool on a power line. (a) Approaching, (b) tool inserting, (c) clamping, (d) releasing. A video of this process can be seen at <http://y2u.be/vDPNLvJjPpo>.

which is most affected by the presence of the attached payload, exhibits a more significant displacement.

These detailed observations and comparisons provide valuable insights into the effectiveness of the control approach, specifically in compensating for the elasticity induced by the payload. By evaluating the differences in motion between the two modalities, the arm's performance and the efficacy of the compensation strategy can be accurately assessed and validated.

6.2 Case Study 2

The second test case has been carried out in the ATLAS Experimental Flight Center⁴ located in the Southern Spain. In this test, the aerial system is perched on a power line cable, while the arm is used to hold a recharging station on the same cable. This is a representative task of the Aerial Core project and, in particular, such a station is used to charge the batteries of the UAV during the inspection operations, exploiting the electricity of the power grid. The weight of the station is around 3.5 kg and consists of a battery charger and two clamps with a housing for the power cable. In addition, the station is actuated in order to close its clamps around the cable. The goal of the aerial manipulator in this case, was to correctly deploy the charger station on the power line. An example of this process is depicted in Figure 8, where the main steps of the task are depicted, from an initial task configuration, to the installation of the device on the cable.

7 CONCLUSIONS

This work introduces a novel design concept for a lightweight manipulator specifically engineered to handle heavy aerial manipulation tasks. One key fea-

ture of this design is the strategic placement of the Center of Mass, situated as close as possible to the arm base. This configuration enhances the arm's portability, making it well-suited for transportation using flying systems.

The primary actuation mechanism employed in this manipulator is based on a set of belts. However, this choice introduces challenges in achieving precise motion at the tip of the manipulator due to the inherent elasticity of the belt system. This behavior becomes particularly prominent when the arm is subjected to heavy payloads. To address this issue, a control approach is proposed to mitigate the effects of elasticity during arm motion. This approach, coupled with the overall system design, aims to optimize the arm's performance and ensure accurate and reliable manipulation tasks.

The main case study for evaluating the proposed arm is within the domain of the Aerial Core EU project. In this project, the aerial arm is specifically employed for inspection and maintenance operations of electrical power grids. This real-world application showcases the practical significance and potential of the proposed system in addressing critical infrastructure challenges.

To validate the effectiveness of the proposed system, both laboratory tests and real-world experiments have been conducted. These experiments include the transportation of a 3.5 kg payload, demonstrating the arm's capability to handle substantial loads and perform precise operations. The results of these tests highlight the system's performance and its potential impact in real-world scenarios.

Moving forward, the future direction of this work involves an extensive evaluation of the arm's capabilities, focusing on more qualitative analysis. This entails further investigations and assessments to comprehensively understand the arm's performance characteristics, enabling refinement and enhancement of its capabilities for a wider range of applications.

⁴<https://atlascenter.aero/en/>

ACKNOWLEDGEMENTS

The research leading to these results has been supported by the AERIAL-CORE project (Horizon 2020 Grant Agreement No. 871479). The authors are solely responsible for its content.

REFERENCES

- Bellicoso, C. D., Buonocore, L. R., Lippiello, V., and Siciliano, B. (2015). Design, modeling and control of a 5-dof light-weight robot arm for aerial manipulation. In *2015 23rd Mediterranean Conference on Control and Automation (MED)*, pages 853–858.
- Cacace, J. and et al. (2021). Safe local aerial manipulation for the installation of devices on power lines: Aerial-core first year results and designs. *Applied Sciences*, 11(13).
- Cacace, J., Finzi, A., Lippiello, V., Furci, M., Mimmo, N., and Marconi, L. (2016). A control architecture for multiple drones operated via multimodal interaction in search rescue mission. In *2016 IEEE International Symposium on Safety, Security, and Rescue Robotics (SSRR)*, pages 233–239.
- Cacace, J., Finzi, A., Lippiello, V., Loianno, G., and Sanzone, D. (2013). Aerial service vehicles for industrial inspection: Task decomposition and plan execution. In Ali, M., Bosse, T., Hindriks, K. V., Hoogendoorn, M., Jonker, C. M., and Treur, J., editors, *Recent Trends in Applied Artificial Intelligence*, pages 302–311, Berlin, Heidelberg. Springer Berlin Heidelberg.
- Cacace, J., Giampetraglia, L., Ruggiero, F., and Lippiello, V. (2023). A novel gripper prototype for helical bird diverter manipulation. *Drones*, 7(1).
- Cano, R., Perez, C., Pruaño, F., Ollero, A., and Heredia, G. (2014). Mechanical design of a 6-dof aerial manipulator for assembling bar structures using uavs.
- Chermprayong, P., Zhang, K., Xiao, F., and Kovac, M. (2019). An integrated delta manipulator for aerial repair: A new aerial robotic system. *IEEE Robotics & Automation Magazine*, 26(1):54–66.
- Franchi, A. (2019). *Platforms with Multi-directional Total Thrust*, pages 53–65. Springer International Publishing, Cham.
- Hamaza, S., Georgilas, I., Fernandez, M., Sanchez, P., Richardson, T., Heredia, G., and Ollero, A. (2019). Sensor installation and retrieval operations using an unmanned aerial manipulator. *IEEE Robotics and Automation Letters*, 4(3):2793–2800.
- IEEE (2009). Guide for maintenance methods on energized power lines. *Std 516-2009*, pages 1–144.
- Joseph, L. and Cacace, J. (2018). *Mastering ROS for Robotics Programming - Second Edition: Design, Build, and Simulate Complex Robots Using the Robot Operating System*. Packt Publishing, 2nd edition.
- Mishra, B., Garg, D., Narang, P., and Mishra, V. (2020). Drone-surveillance for search and rescue in natural disaster. *Computer Communications*, 156:1–10.
- Miyazaki, R., Paul, H., Kominami, T., and Shimonomura, K. (2020). Wire-suspended device control based on wireless communication with multirotor for long reach-aerial manipulation. *IEEE Access*, 8:172096–172104.
- Ollero, A., Tognon, M., Suarez, A., Lee, D., and Franchi, A. (2022). Past, present, and future of aerial robotic manipulators. *IEEE Transactions on Robotics*, 38(1):626–645.
- Paul, H., Miyazaki, R., Ladig, R., and Shimonomura, K. (2019). Landing of a multirotor aerial vehicle on an uneven surface using multiple on-board manipulators. In *2019 IEEE/RSJ International Conference on Intelligent Robots and Systems (IROS)*, pages 1926–1933.
- Ruggiero, F., Lippiello, V., and Ollero, A. (2018). Aerial manipulation: A literature review. *IEEE Robotics and Automation Letters*, 3(3):1957–1964.
- Shimahara, S., Leewiwatwong, S., Ladig, R., and Shimonomura, K. (2016). Aerial torsional manipulation employing multi-rotor flying robot. In *2016 IEEE/RSJ International Conference on Intelligent Robots and Systems (IROS)*, pages 1595–1600.
- Sibanyoni, S. V., Ramotsoela, D. T., Silva, B. J., and Hancke, G. P. (2019). A 2-d acoustic source localization system for drones in search and rescue missions. *IEEE Sensors Journal*, 19(1):332–341.
- Suarez, A., Heredia, G., and Ollero, A. (2018). Design of an anthropomorphic, compliant, and lightweight dual arm for aerial manipulation. *IEEE Access*, 6:29173–29189.
- Suarez, A., Nekoo, S. R., and Ollero, A. (2023). Ultra-lightweight anthropomorphic dual-arm rolling robot for dexterous manipulation tasks on linear infrastructures: A self-stabilizing system. *Mechatronics*, 94:103021.
- Suarez, A., Real, F., Vega, V. M., Heredia, G., Rodriguez-Castaño, A., and Ollero, A. (2020). Compliant bimanual aerial manipulation: Standard and long reach configurations. *IEEE Access*, 8:88844–88865.
- Tognon, M., Chávez, H. A. T., Gasparin, E., Sablé, Q., Bicego, D., Mallet, A., Lany, M., Santi, G., Revaz, B., Cortés, J., and Franchi, A. (2019). A truly-redundant aerial manipulator system with application to push-and-slide inspection in industrial plants. *IEEE Robotics and Automation Letters*, 4(2):1846–1851.
- Tosato, P., Facinelli, D., Prada, M., Gemma, L., Rossi, M., and Brunelli, D. (2019). An autonomous swarm of drones for industrial gas sensing applications. In *2019 IEEE 20th International Symposium on "A World of Wireless, Mobile and Multimedia Networks" (WoW-MoM)*, pages 1–6.
- Trujillo, M. A., Martinez-de Dios, J. R., Martin, C., Viguria, A., and Ollero, A. (2019). Novel aerial manipulator for accurate and robust industrial ndt contact inspection: A new tool for the oil and gas inspection industry. *Sensors*, 19(6).
- Uzakov, T., Nascimento, T. P., and Saska, M. (2020). Uav vision-based nonlinear formation control applied to inspection of electrical power lines. In *2020 International Conference on Unmanned Aircraft Systems (ICUAS)*, pages 1301–1308.